Adapting Stiffness and Attack Angle through Learning Rule Sets to Increase Self-Stability in Locomotion

Kathryn Walker[1,2,*], Helmut Hauser[1,2]

[1] *University of Bristol, Bristol, BS8 1TH*
[2] *Bristol Robotics Laboratory, Stoke Gifford, Bristol BS16 1QY*
kw16876@bristol.ac.uk
[*] *Corresponding Author*

Abstract

Biological systems are outperforming machines in legged locomoting under almost any conditions. This is partly due to their capability of learning from failure and adapting their control approach and morphological features. This paper proposes an approach that extends the spring-loaded inverted pendulum (SLIP) model with the capability to adapt its attack angle (control) and stiffness (morphology) based on previous locomotion attempts. A set of different update rules, i.e., how this experience is used to adapt, are systematically investigated. The results suggest that modifying either attack angle, or stiffness, or both is beneficial with respect to achieve stable locomotion. Particularly, if the current system configuration (control and morphology) outperforms the previous one, the results suggest that increasing the angle and decreasing the stiffness of the system leads to more stable solutions. Consequently, the basic SLIP model extended by the proposed learning capabilities is able to reach stable locomotion over a much wider range of parameter combinations simply through trial and error.

Keywords: Learning; Legged locomotion; Trial and Error; SLIP Model; Control; Morphology

Word Count: 3229

1. Introduction

Despite the huge success of robotics in general, there are almost no machines that are capable to stably locomote in rough, unknown terrain. As a consequence, most of today's robots work only in well-defined environments like assembly lines and on the factory floor. Even state-of-the-art robots are still not able to deal with the uncertainty, complexity and variety typical of natural environments and our living and working places. Simply put, if they can't model it, they'll fail. On the other hand, animals, including us humans, are particularly good at locomotion and we outperform robots in almost any category, including, energy efficiency, stability, robustness, agility, and many others [1][24]. This is partly due to the fact that a lot of the locomotion process happens without the need of an exact model of the environment. For example, part of self-stabilisation can be carried out by the morphological structure of the legs. One could say control is outsourced to the morphology. In robotics, this is often referred to as morphological computation [9, 10, 8]. Another important difference is that animals are remarkable adaptive. They can locomote over a wide range of different terrains [23, 11, 5, 4]. Key properties are their capability of learning from previous experience and their capacity to adapt, i.e., change their control strategy and/or change their morphological properties, e.g., like adapting stiffness). While numerous mechanisms have been proposed to adapt stiffness, typically referred to as variable compliant mechanisms [22, 25], only few have been used to actively increase locomotion performance. For example, Quy et al. used adaption of stiffness to improve energy efficiency in single-legged hopper [23].

In this work we propose an approach that implements these learning and adaptation capabilities on the well-established spring-loaded inverted pendulum model (SLIP) model, which is a prevalent model for analyzing running and hopping [2]. This simple model is surprisingly general as it works over a wider range of species and locomotion types. In its basic form it describes the action of the leg by representing it as a lossless, linear spring of constant stiffness k and rest

length l_o as shown in Figure 1. The leg has no mass and the body is represented by a point mass. The SLIP model is self-stabilizing, i.e., the system can tolerate small perturbations without loosing its periodic locomotion pattern[6]. Seyfarth et al. showed the range of stiffness and angle combinations that resulted in self-stability for a simple SLIP model [20, 7].

Many researchers have tried to find ways to widening this self-stabilizing region. Some have adapted the control of the SLIP model, such as Seyfarth et al. [21, 19] who use the stiffness and horizontal velocity values to influence the retraction of the leg during the flight phase and thus change the attack angle at touch down. Similarly, Schmitt [18] changes the attack angle based on the angle at lift off and desired angle.

Another adopted approach is to change the morphology (stiffness) of the model. Owaki et al. investigated different nonlinear stiffness function and identified the ones that are beneficial [15]. Similiary, Karssen et al. [13] optimized offline the stiffness function with respect to disturbance rejection. Also using increasing the number of leg segments, like in [16] and [17], lead to nonlinear stiffness functions and a bigger region of self-stabilization.

Blum et al. [3] combined both previously mentioned methods by adding control strategies to change both angle and stiffness in the flight phase, ready for touch down. Iida et al. [12] use reinforcement learning to tune the motor frequency of a one legged robot based on the SLIP model.

While all these approaches are able to widen the region of stable pairs of attack angle and stiffness, they don't allow to learn from unsuccessful starting parameter (stiffness/attack angle) combinations. If these starting parameters are outside the area of self-stability there is no possibility of becoming stable.

We propose a method that allows the SLIP model to adapt its attack angle (control parameter) and stiffness (morphological parameter) based on change in kinetic energy between strides through use of learning rules. This approach has a great potential to be used in variety of applications where learning/adaption over time is necessary. This ranges from locomotion rehabilitation devices to helping stroke patients, to supportive walking devices for elderly, to adaptive,

autonomous, legged robots. In all these cases, there is a need for learning to adapt to changes in either the human user (e.g. due to improvement through training or deterioration by aging) or the robot and environment (due to wear or changes in the ground dynamics) .

In the next section, we briefly explain the SLIP model and described the used methodology. In Section 3 we present results and discuss their implications in the Section 4. Finally, we present a future outlook.

2. Method

2.1. The SLIP model

Insert Figure 1 here

This SLIP model has been introduced in [2] (and discussed further in [14]) as generic model of legged locomotion. Historically, the movement of the leg is formed of two phases; the flight phase and the stance phase, as shown in Figure 1. We follow the simulation layout from [21].

The leg was simulated in Matlab using the Forward Euler method for integration with a time step of $\Delta t = 0.001$ seconds. The SLIP model was simulated until either the leg fell over (the vertical height of the mass was less than ground level, i.e. $y < 0$) or the maximum time of $t = 10$ seconds ($= 10'000$ simulation time steps) was achieved. If the leg had not fallen over after 10 seconds it was considered stable. For this paper, the time from the point the leg is starting to move to when it falls over or it reaches 10 seconds is called as an *episode*. Therefore, the maximum length of one episode is 10 seconds. Note that potentially there are parameter combinations that could lead to falling over after 10 seconds. However, we found that 10 seconds for the duration of an episode was a reasonable trade-off between simulation time and stability. Since, our approaches allows to learn from previous experience, e.g. either from a failed episode of $t < 10$ seconds or from a successful episode, we assume the model can "get up" again and start with slightly changed parameters (either different attack angle α or stiffness k, or both). We allow the simulation to run a total of

100 episodes to learn from experience. This 100 episodes are referred to as one life time. Similiarly to our choice for the duration of one episode, a life time of 100 episodes was found, after some testing, to be a reasonable trade-off between simulation time and stability. The resting length of the leg in the simulation was 1 m, the point mass was 80 kg. This is consistent with the values used in literature, see [21].

2.2. Rule Set Design

This section introduces the basic set of rules that was used to learn from one episode to another. Depending on the rules the SLIP model will either change the attack angle α, the stiffness k, or both. We systematically investigate all possible combinations of this basis rule set to obtain the best solutions. The goal was to have a SLIP model that can, through learning from failure and corresponding adaptation, reach stable solutions. The generic rule set as well as an example rule set are shown in Figure 2.

Insert Figure 2 here

The sets of rules for exploring the adaptation of attack angle and stiffness are similar. Each set consists of five individual rules. At the end of each episode the adaptation is based on the achieved distance D_i and the distance achieved in the previous episode D_{i-1}. Note that for a successful run the achieved distance is the distance the SLIP model has traveled after 10 s. For an unsuccessful run it is the distance traveled before model has fallen over.

The key parameter for the adaptation process is the difference between these two distances, i.e., $\Delta D = D_i - D_{i-1}$.

The first rule dictates whether, upon a positive ΔD, the parameter (either α or k) should increase or decrease. Symmetry is employed, so if ΔD is negative the opposite occurs. Rule 2 dictates whether, when the parameter is to *increase*, this increase should be dependent on ΔD or a fixed value. Similarly, Rule 3 dictates whether, when the parameter is to *decrease*, this amount should be fixed or unfixed.

If the parameter change is *unfixed* (regardless of whether it is increasing/decreasing

or) the algorithm uses following Equation to calculate the parameter change.

$$\text{parameter change} = \frac{\mu}{2 + \Delta D}, \tag{1}$$

where $\Delta D = D_i - D_{i-1}$ and μ is given by A4/S4. Note that if A3/S3 is unfixed, A5/S5 is redundant. The parameter change is then added or removed from the current parameter depending on Rules 2/3.

If a fixed value is to be used Rules 4 and 5 dictate this value, 4 if the new parameter configuration has performed better, 5 if it has performed worse[1]. If the parameter is changed according to the rules to a value that is outside of the range ($< 0°$, $> 90°$ or a negative stiffness) the learning process is terminated (the lifetime is finished) and the rule set is determined unsuitable.

Based on these basic rules, we investigated all possible combinations. Considering that Rules A1, A2, and A3 are binary (i.e., either fixed/unfixed or increase/decrease) and we explored Rule A4 and Rule A5 for values from 0.01 to 0.9 in 10 discretitized steps, we investigated at total of $2^3 * 10 * 10 = 800$ combinations (see for example Figure 4A). The same number of different rule set were explored for the stiffness adaptation using Rules S1-S5.

For each of the 800 combinations we systematically tested a wide range of possible pairs of attack angles α and stiffness values k. The range encompassed for α, values from $20°$ to $90°$ (in 40 discrete steps) and for k from $2,000$ to $60,000$ N/m (also in 40 discrete steps). This results in 1,600 different angle/stiffness pairs. Note that this range (i.e., lower and upper bounds) has been chosen pragmatically; first, to fully encompassed the stability region as determined by [20] and, second, to explore enough interesting parameter combination to demonstrate the validity as well the limitations of our approach. For a given set of rules we simulated the model with all 1,600 different starting pairs and observed if the system was able to achieve stable locomotion through applying the rule over a lifetime (i.e., over 100 episodes).

[1]Note that varying stiffness rules S4 and S5 are multiplied by a factor of 10^4 to allow for the difference in magnitude between stiffness and attack angle.

To assess whether a rule set is good or not, a *success rate* was defined. The *success rate* the percentage out of all $1,600$ possible starting points that lead to a stable solution (in percentage) applying the learning rules. For example, if a rule set would be able to find a stable solution for all $1,600$ combination, it would have a success rate of 100%. Since we use the same number of simulations for all rules, we can quantitatively compare them within the explored parameter range. Note that the *success rate* gives us a comparative measurement on the usefulness of any given set of learning rules. The higher the *success rate*, the bigger is the region of parameter combinations that our set of learning rules can recover from, i.e. it can lead successfully the system through learning to the stable region in the parameter space. This behaviour is particularly useful if we have to deal with real systems that change their dynamics, e.g. changes in stiffness due to age or failure.

3. Results

3.1. The Baseline: SLIP with No Parameter Changes

First, we simulated the standard SLIP model (i.e., no online adapdation of parameters) to establish a baseline. We tested the model over the previously described 1,600 angle and stiffness combinations. Since no learning was included the stiffness and angle parameters were unable to change.

Figure 3 shows the performance. A pink dot indicates a starting condition where a stable solution could not be obtained throughout the model's life time. The figure clearly shows that a standard SLIP model only a small set of stiffness/angle combinations are leading to stable locomotion. This area of stability is in literature often referred as J-Figure (e.g., [20].) The success rate for the non-learning SLIP model was 3.75% (60 out 1600 parameter pairs were stable).

Insert Figure 3 here

3.2. Adapting the Attack Angle

This section describes the result from testing rules that change the attack angle α. Every combination (a total of 800) was tested and the results in form of success rates are presented in Figure 4. Table 1 summarizes the top 5 rule sets (they are also highlighted in red in Figure 4A). The best rule obtained a success rate of 78.93%, which is much higher compared to the standard SLIP model with 3.75% (the corresponding base line is the red line in Figure 4A).

Insert Table 1 here

Insert Figure 4 here

The top scoring rule sets from Table 1 all follow a similar learning mechanism. If the current distance D_i is larger than the previously achieved distance D_{i-1} the angle of attack is increased. The amount is inversely proportional to δD. This allows the agent to climb the gradient of the SLIP model without overshooting the global optimum (which is in the J-Figure). Accordingly, if the leg performance was worse than the the previous run, i.e., $\Delta D < 0$, the angle was reduced by a fixed amount.

Figure 4A also shows that any combination of our proposed rules for changing the attack angle is performing better than the default SLIP model, i.e., all success rates are higher than the base line in red. Similar to the Figure 3 we tested all starting combinations of α and k for the best rule set, see Figure 4B. It can been seen clearly that the region that leads to stable solutions is much bigger (success rate 78.93%) compared to the standard SLIP (success rate 3.75%, see Figure 3). But there are also some limitations visible in Figure 4B. It seems for starting points left to the J-figure (i.e., smaller angles) most of the points reach a stable solution (i.e., not a pink dot), while on the right side (higher angle values) the performance is limited. To further investigate that we looked at starting parameters specifically on the right side and on the left side and observed the change of α over time. If the starting angle is on the right hand side of the J-Figure, the learning mechanism will zig-zag away from the optimal region.

By looking at the underlying gradient we can see that either side of the peak

stability region the gradient is negative. Consequently, when on the right side of the solution the update rules will lead away from the stable region, see Figure 5B.

Insert Figure 5 here

Given this gradient arrangement, a rule set that would be able to distinguish between "left" and "right" would perform even better. However, our proposed setup did not allow for this, because we assume the system does not have the information in which direction the stable region is located. Another problem starting point area is shown by the red circle in Figure 4B. By looking at the development of the attack angle over time we observed oscillation between an angle slightly below the stable region and one slightly above it. Interestingly, this behaviour is unique to the top rule set and is not observed in the other top 4 rules listed in Table 1. However, the other rules have lower success rates due more unstable points on the right-hand side (i.e., at higher attack angles).

3.3. Adapting the Stiffness

In addition to the angle changing rule set testing, we also tested 800 stiffness changing rule. Figure 6A summarizes the obtained success rates. Table 2 shows the top 5 stiffness changing rule sets.

Insert Table 2 here

Insert Figure 6 here

For the best stiffness adaptation rule we plotted the region of success starting points, see Figure 6B. The corresponding success rate was 51%. One can see that the parameter regions that lead to stable solutions is much bigger than for the SLIP without learning (compare Figure 3, success rate 3.75%), but it's smaller compared to the best angle adaptation rule (see Figure 4, success rate 78.93%). Again, any of the tested adaptation rules performs better than the standard SLIP model with fixed parameters (compare red baseline in Figure 4A).

As with the angle changing rule sets, the top five stiffness changing rule sets all

follow the same three starting rules. The stiffness value is increased if the leg performs better than in the previous episode $\Delta > 0$, and decreased if $\Delta D < 0$. Both the increase and decrease of the stiffness is fixed regardless of the magnitude of ΔD.

In contrast to the attack angle adaptation rule sets, where one rule seems to stand out with respect to performance, for stiffness adaptations there seems be various rule sets with the different first three rules (for example *[Decrease, Fixed, Fixed]*, and even *[Decrease, Unfixed, Fixed]*, see Figure 6A) that are also very successful.

3.4. Adapting and Attack Angle and Stiffness Simultaneously

Finally, the adaptation of both, attack angle and stiffness, was investigated. Due to the high number of possible combinations (640,000) not every single possible rule set was tested. In fact, it would take just under 1 year of simulation time to complete all this testing. Instead a simpler approach was taken.

First, a stiffness and angle changing rule set was created by combining the best angle changing rule set (Table 1) with the best stiffness changing rule set (Table 2), i.e. *[Increase, Unfixed, Unfixed, 0.67, 0.23]* for adapting the attack angle, and *[Increase, Fixed, Fixed, 0.89, 1]* for adapting the stiffness. Figure 7 shows the corresponding performance. The success rate was 75.56%, which is a little bit lower than the the best angle adaptation rule (78.93%), but higher than the best stiffness adaptation rule (51.0%).

Insert Figure 7 here

Although the overall success rate of the combined rule set is lower than the top angle changing rule set, an advantage of this combination is that the the problem area shown in Figure 9 does not show here. A disadvantage of this combination is the region highlighted by the black circle in Figure 7, which seems to emergence because of the combination. In this case the stiffness and angle change work against each other. The changes they introduce have opposite effects resulting in a zig-zag pattern in a direction perpendicularly away from the area of stability. This suggests that the approach of simply combing the best

angle attack and stiffness adaptation rule sets is rather naive. Nevertheless, potentially, there are other combinations that perform better. Due to the huge search space we only tested combinations of all our top 5 rules (i.e. 25 combinations). The summary of the top five combinations can be found in Table 3. Interestingly, they all use the best angle rule set, but use inferior stiffness rule sets to achieve higher success rates.

Insert table 3 here

4. Discussion and Further Work

This paper demonstrates that by allowing the SLIP model to learn from previous experience, it is able to recover from a much wider range of possible starting combinations of control parameter (attach angle) and morphological parameter (spring stiffness). This adds a new level of adapativity with the great potential to use it in a wide range of applications. For example, the approach could be employed in rehabilitation devices to help stroke patients, where stable walking is often a challenge. Another application could be supportive walking devices (e.g. exoskeleton) for elderly who are particularly prune to falling over. Having a SLIP-model-based machine capable of adapting itself over time (i.e during a training phase supervised by a medical professional) would significantly improve the performance. Furthermore, it would be able to adapt itself over time in case of degenerative diseases, where locomotion capabilities of the user naturally decreases over time. In addition, the same approach would beneficial in the context of autonomous locomotion for robotic systems, e.g., in changing environments or changes in the dynamics due to extensive use.

Our results suggest that updating the angle is more successful in achieving robust locomotion than changing the stiffness. This is due to the fact that the angle rules establish a much steeper gradient close to the region of stability, compared to the one based on stiffness. Therefore, changing the angle has a bigger, positive effect (i.e., getting faster to the region of stability). This be-

came particularly obvious when we combined the top stiffness and the top angle changing rule sets. Furthermore, even adding small angle change to any given stiffness rule improved the success rate significantly.

In this work we have only explored a small number of possible rule sets and combination with a *brute force* approach. While the presented results are encouranging, various nonlinear optimization approaches, like Genetic Algorithms, cleary could be used to explore a much bigger space of combination and possible rules. This will be a part of future work.

5. Figures

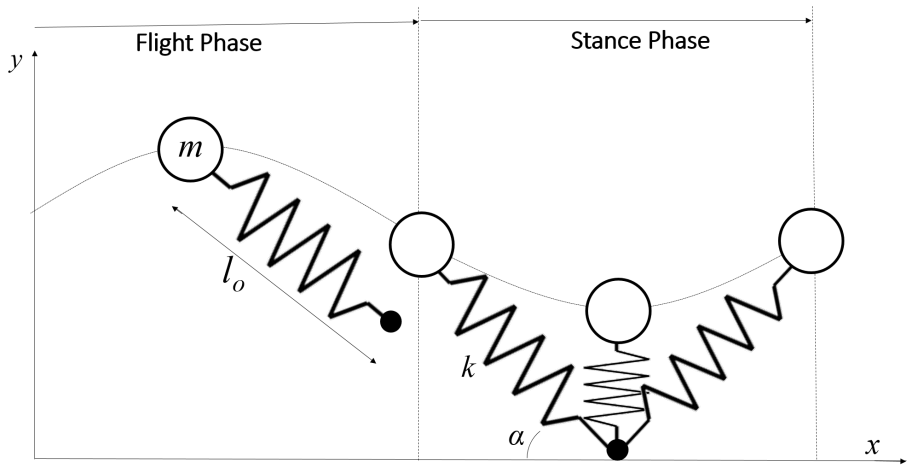

Figure 1: Figure shows the two stages in the SLIP model – flight and stance. During the flight phase the length of the massless spring remains constant and the pendulum follows a ballistic trajectory until the foot comes in contact with ground level. During stance phase the foot position of the leg remains constant. The mass rotates around the foot position driven by the kinetic energy of the mass. The model switches to flight phase again, when the spring has reached it's resting length represented by l_o. Other parameters the mass m, the stiffness k, and the attack angel α.

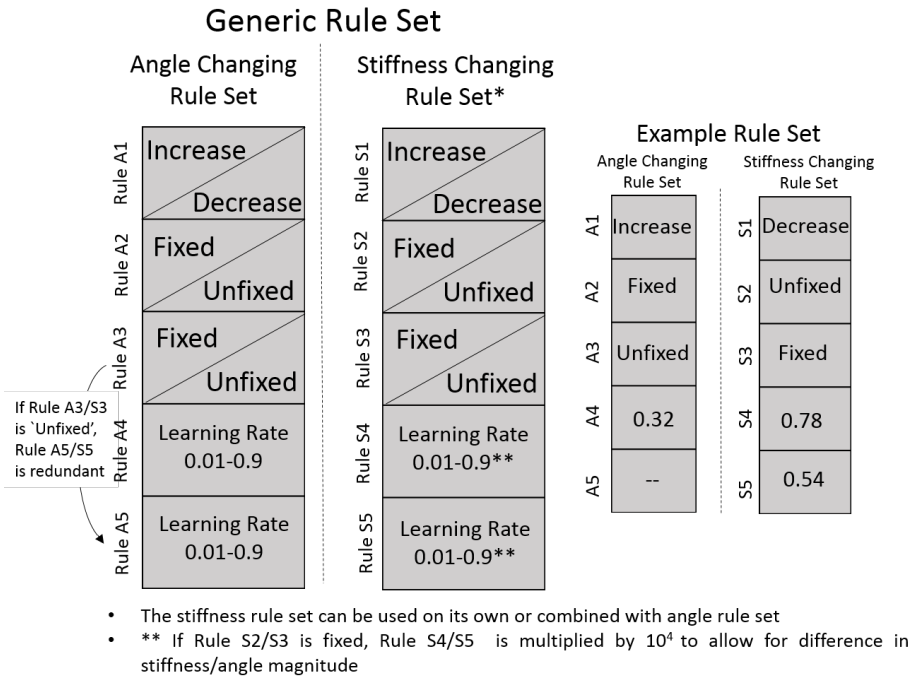

Figure 2: Generic rule set used throughout this paper. The left side show the set of rules to adapt the attack angle α (rules A1-A5) and the right to adapt stiffness k (rules S1-S5). The figure also shows the range for the different rules. Note that Increase/Decrease and Fixed/Unfixed are binary. Also included in this figure is an example rule set for added clarity.

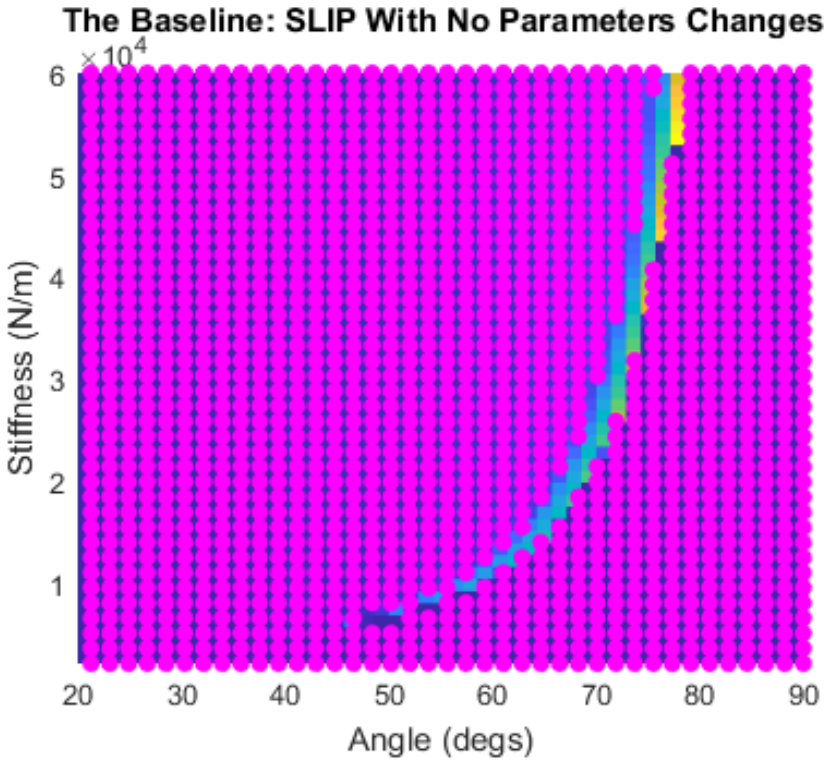

Figure 3: Figure shows the amount of stable parameter combinations for all possible attack angle and stiffness for basic SLIP model that does not adapt its parameters. A pink dot indicates that no stable solution could be found with this starting position. It can be seen that such a fixed SLIP model has very few stable starting points. The color coding in the background reflects the average traveled distance for this given angle/stiffness combination. The lighter the color the further it was able to locomote.

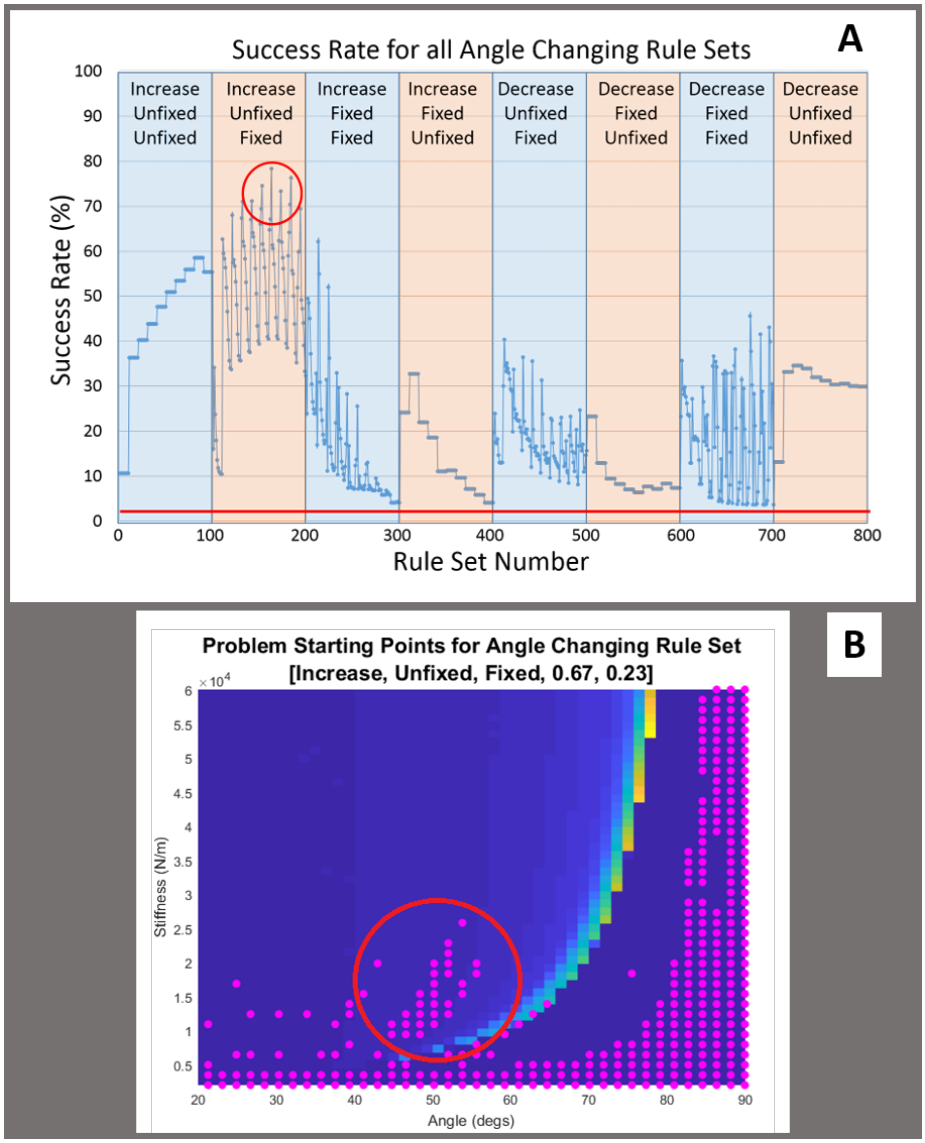

Figure 4: A) shows the success rate (as defined in the text) for all 800 tested angle changing rule sets. Each column represents 100 rule sets that share the same first three binary rules. The red circle shows the location of the best sets of rules that are also detailed in Table 4. The red line on the bottom shows the base line success rate (i.e. the success rate for a non-learning model, see Figure 3). Areas of similar success rates seen in 1st, 4th, 6th and 8th columns are due to the redundancy of the Rule A5 in these cases. It should be noted that the difference between the stepped and spikey patterns is due to the particular arrangement of the rule sets. If the rules were sorted differently a different arrangements of patterns would be seen. B) shows the performance of the best angle changing rule set *[Increase, Unfixed, Fixed, 0.67, 0.23]*. A pink dot indicates that no stable solution could be found with this starting position. The red circle highlights an area of unexpected problem starting points discussed in the text.

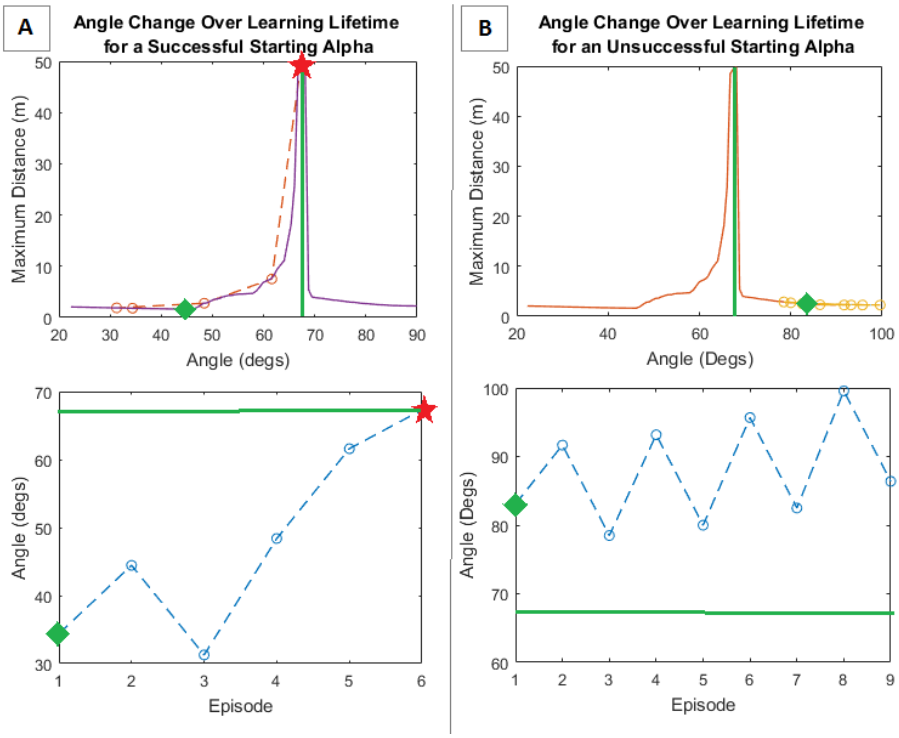

Figure 5: The graphs show how the top angle changing rule set attempts learn a stable solution. The top figures shows how the rule adapts its angles over multiples steps with respect to the underlying cost function landscape. The bottom graphs show how the angle is changed over time. A) shows results for a successful starting angle. B) shows results for an unsuccessful starting position (from a pink dot). In both cases the green diamond indicates the start position, a red star the final position. The stiffness in both cases is kept constant at 20,000 N/m. The green lines on the bottom graphs show the angle where the model would be stable.

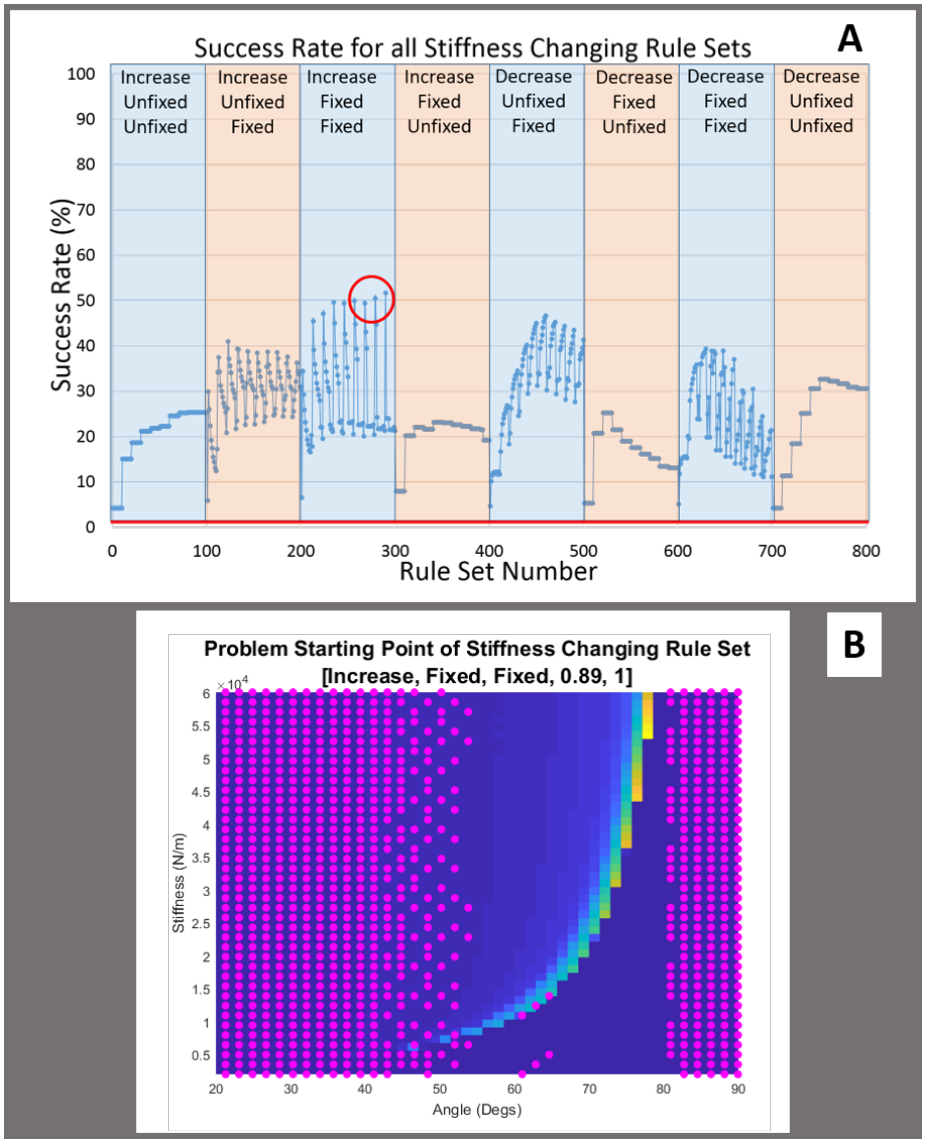

Figure 6: A) shows the success rate (as defined in the text) for all 800 tested stiffness changing rule sets. Each column represents 100 rule sets that share the same first three binary rules. The red circle shows the location of the best sets of rules that are also detailed in Table 4. The red line on the bottom shows the base line success rate (i.e. the success rate for a non-learning model, see Figure 3). Areas of similar success rates seen in 1st, 4th, 6th and 8th columns are due to the redundancy of the Rule S5 in these cases.It should be noted that the difference between the stepped and spikey patterns is due to the particular arrangement of the rule sets. If the rules were sorted differently a different arrangements of patterns would be seen. B) Performance of the best angle changing rule set *[Increase, Fixed, Fixed, 0.89, 1]*. A pink dot indicates that no stable solution could be found with this starting position.

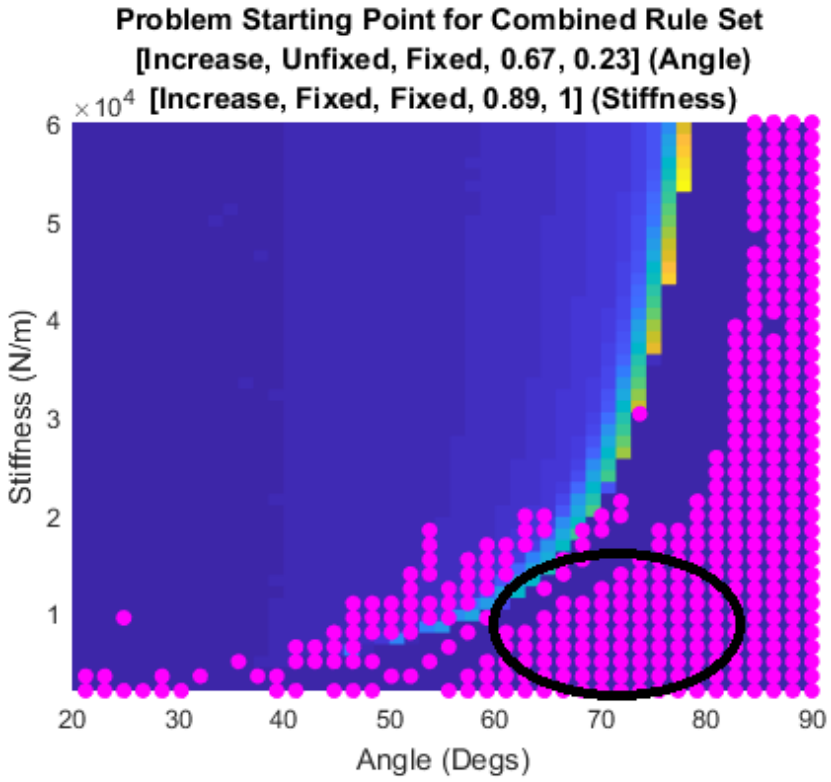

Figure 7: Performance when the best stiffness and angle changing rule sets are combined, i.e., *[Increase, Unfixed, Fixed, 0.67, 0.23 (angle) Increase, Fixed, Fixed, 0.89, 1 (stiffness)]*. The black circle highlights an interesting area of unexpected problem starting points. See text for discussion.

6. Tables

Rule Set	Success Rate
Increase, Unfixed, Fixed, 0.67, 0.23	78.93%
Increase, Unfixed, Fixed, 0.78, 0.23	73.91%
Increase, Unfixed, Fixed, 0.45, 0.12	71.12%
Increase, Unfixed, Fixed, 0.34, 0.12	71.12%
Increase, Unfixed, Fixed, 0.56, 0.12	69.31%

Table 1: Top 5 successful angle changing rule sets and their corresponding success rates. These top rules can also be seen in Figure 4 within the red circle.

Rule set	Success Rate
Increase, Fixed, Fixed, 0.89, 1.00	51.0%
Increase, Fixed, Fixed, 0.78, 0.89	50.5%
Increase, Fixed, Fixed, 0.56, 0.67	49.9%
Increase, Fixed, Fixed, 0.45, 0.56	49.3%
Increase, Fixed, Fixed, 0.67, 0.78	49.3%

Table 2: Top 5 successful stiffness changing rule set and their corresponding success rates. These top rules can also be seen in Figure 6 within the red circle.

7. Acknowledgements

This work was supported by the EPSRC Centre for Doctoral Training in Future Robotics and Autonomous Systems (FARSCOPE) EP/L015293/1. The research was also partly supported by the Leverhulme Trust Research Grant RPG-2016-345.

8. Conflict of Interests

We, the authors, declare that we have no financial or personal relationships with other people or organizations that could inappropriately influence (bias)

Angle Rule Rank	Stiffness Rule Rank	Success Rate
1	4	76.31%
1	3	76.31%
1	2	76.25%
1	5	75.81%
1	1	75.56%

Table 3: Table showing top 5 of the 25 different rule set combinations tested

our work.

References

[1] Alexander, R. M. (2003). *Principles of animal locomotion*. Princeton University Press.

[2] Blickhan, R. (1989). The spring-mass model for running and hopping. *Journal of Biomechanics*, 22(11-12):1217–1227.

[3] Blum, Y., Lipfert, S. W., Rummel, J., and Seyfarth, A. (2010). Swing leg control in human running. *Bioinspiration & Biomimetics*, 5(2):026006.

[4] Cham, J. G., Karpick, J. K., and Cutkosky, M. R. (2004). Stride period adaptation of a biomimetic running hexapod. *The International Journal of Robotics Research*, 23(2):141–153.

[5] Dickinson, M. H., Farley, C. T., Full, R. J., Koehl, M., Kram, R., and Lehman, S. (2000). How animals move: an integrative view. *science*, 288(5463):100–106.

[6] Ernst, M., Geyer, H., and Blickhan, R. (2010). Spring-legged locomotion on uneven ground: a control approach to keep the running speed constant. In *Mobile Robotics: Solutions and Challenges*, pages 639–644. World Scientific.

[7] Geyer, H., Blickhan, R., and Seyfarth, A. (2002). Natural dynamics of spring-like running: Emergence of selfstability. In *5th International Conference on Climbing and Walking Robots*, pages 87–91. Suffolk, England: Professional Engineering Publishing Ltd.

[8] Hauser, H., Füchslin, R. M., and Pfeifer, R. (2014). Opinions and outlooks on morphological computation.

[9] Hauser, H., Ijspeert, A. J., Füchslin, R. M., Pfeifer, R., and Maass, W. (2011). Towards a theoretical foundation for morphological computation with compliant bodies. *Biological cybernetics*, 105(5-6):355–370.

[10] Hauser, H., Ijspeert, A. J., Füchslin, R. M., Pfeifer, R., and Maass, W. (2012). The role of feedback in morphological computation with compliant bodies. *Biological cybernetics*, 106(10):595–613.

[11] Hurst, J. W. and Rizzi, A. A. (2005). Physically variable compliance in running. In *Climbing and Walking Robots*, pages 123–133. Springer.

[12] Iida, F. and Tedrake, R. (2007). Motor control optimization of compliant one-legged locomotion in rough terrain. In *Intelligent Robots and Systems, 2007. IROS 2007. IEEE/RSJ International Conference on*, pages 2230–2235. IEEE.

[13] Karssen, J. D. and Wisse, M. (2011). Running with improved disturbance rejection by using non-linear leg springs. *The International Journal of Robotics Research*, 30(13):1585–1595.

[14] McMahon, T. A. and Cheng, G. C. (1990). The mechanics of running: how does stiffness couple with speed? *Journal of biomechanics*, 23:65–78.

[15] Owaki, D. and Ishiguro, A. (2006). Enhancing self-stability of a passive dynamic runner by exploiting nonlinearity in the leg elasticity. In *SICE-ICASE, 2006. International Joint Conference*, pages 4532–4537. IEEE.

[16] Rummel, J., Iida, F., Smith, J. A., and Seyfarth, A. (2008). Enlarging regions of stable running with segmented legs. In *2008 IEEE International Conference on Robotics and Automation*, pages 367–372.

[17] Rummel, J. and Seyfarth, A. (2008). Stable running with segmented legs. *The International Journal of Robotics Research*, 27(8):919–934.

[18] Schmitt, J. (2006). A simple stabilizing control for sagittal plane locomotion. *Journal of Computational and Nonlinear Dynamics*, 1(4):348–357.

[19] Seyfarth, A. and Geyer, H. (2002). Natural control of spring-like running–optimized self-stabilization. In *Proceedings of the Fifth International Conference on Climbing and Walking Robots. Professional Engineering Publishing Limited*, pages 81–85.

[20] Seyfarth, A., Geyer, H., Günther, M., and Blickhan, R. (2002). A movement criterion for running. *Journal of Biomechanics*, 35(5):649–655.

[21] Seyfarth, A., Geyer, H., and Herr, H. (2003). Swing-leg retraction: a simple control model for stable running. *Journal of Experimental Biology*, 206(15):2547–2555.

[22] Vanderborght, B., Albu-Schäffer, A., Bicchi, A., Burdet, E., Caldwell, D. G., Carloni, R., Catalano, M., Eiberger, O., Friedl, W., Ganesh, G., et al. (2013). Variable impedance actuators: A review. *Robotics and autonomous systems*, 61(12):1601–1614.

[23] Vu, H. Q., Hauser, H., Leach, D., and Pfeifer, R. (2013). A variable stiffness mechanism for improving energy efficiency of a planar single-legged hopping robot. In *Advanced Robotics (ICAR), 2013 16th International Conference on*, pages 1–7. IEEE.

[24] Wieber, P.-B., Tedrake, R., and Kuindersma, S. (2016). Modeling and control of legged robots. In *Springer handbook of robotics*, pages 1203–1234. Springer.

[25] Wolf, S., Grioli, G., Eiberger, O., Friedl, W., Grebenstein, M., Höppner, H., Burdet, E., Caldwell, D. G., Carloni, R., Catalano, M. G., et al. (2016). Variable stiffness actuators: Review on design and components. *IEEE/ASME transactions on mechatronics*, 21(5):2418–2430.